

Nitric Oxide Is Reduced to HNO by Proton-Coupled Nucleophilic Attack by Ascorbate, Tyrosine, and Other Alcohols. A New Route to HNO in Biological Media?

Sebastián A. Suarez,[†] Nicolás I. Neuman,^{†,‡} Martina Muñoz,[†] Lucia Alvarez,[†] Damián E. Bikiel,[†] Carlos Brondino,[‡] Ivana Ivanović-Burmazović,[§] Jan Lj. Miljkovic,[§] Milos R. Filipovic,[§] Marcelo A. Martí,^{*,†,⊥} and Fabio Doctorovich^{*,†}

[†]Departamento de Química Inorgánica, Analítica y Química Física, Facultad de Ciencias Exactas y Naturales, Universidad de Buenos Aires, Ciudad Universitaria/INQUIMAE-CONICET, Buenos Aires, Argentina

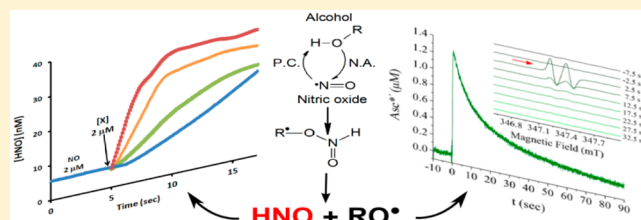
[‡]Departamento de Física, Facultad de Bioquímica y Ciencias Biológicas, Universidad Nacional del Litoral, Ciudad Universitaria, Paraje El Pozo, Santa Fe, Argentina

[§]Department of Chemistry and Pharmacy, Friedrich-Alexander University Erlangen-Nuremberg, Egerlandstrasse 1, 91058 Erlangen, Germany

[⊥]Dr. Marcelo A. Martí. Departamento de Química Biológica, FCEN, UBA, Ciudad Universitaria, Pab. II, 1428, Buenos Aires, Argentina

Supporting Information

ABSTRACT: The role of NO in biology is well established. However, an increasing body of evidence suggests that azanone (HNO), could also be involved in biological processes, some of which are attributed to NO. In this context, one of the most important and yet unanswered questions is whether and how HNO is produced in vivo. A possible route concerns the chemical or enzymatic reduction of NO. In the present work, we have taken advantage of a selective HNO sensing method, to show that NO is reduced to HNO by biologically relevant alcohols with moderate reducing capacity, such as ascorbate or tyrosine. The proposed mechanism involves a nucleophilic attack to NO by the alcohol, coupled to a proton transfer (PCNA: proton-coupled nucleophilic attack) and a subsequent decomposition of the so-produced radical to yield HNO and an alkoxy radical.



INTRODUCTION

After over two decades of intense research, the chemical reactivity of nitric oxide and its key roles in several biological processes, including cardiovascular regulation, immune response, and neuronal physiology are, in principle, well established.^{1–4} Azanone (HNO/NO⁻), also called nitroxyl, is the one electron reduction product of NO and its reactivity and biological relevance are currently under intense debate.^{5–8} It dimerizes rapidly ($k_{\text{dim}} = 8 \times 10^6 \text{ M}^{-1} \text{ s}^{-1}$),⁹ which limits its concentration and lifetime in the solution. Moreover, HNO reacts quickly with its sibling NO ($k = 5.6 \times 10^6 \text{ M}^{-1} \text{ s}^{-1}$)¹⁰ and at a moderate rate ($k = 3 \times 10^3 \text{ M}^{-1} \text{ s}^{-1}$) with oxygen.^{9,11,12}

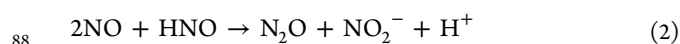
HNO signaling is distinct to that of NO: HNO reacts mainly with thiols^{8,13} and heme Fe(III) centers.^{14,15} Unlike NO, HNO activates HNO-TRPA1-CGRP signaling cascade for the regulation of blood pressure and control of cardiac contractility.⁵ The lack of certainty concerning its endogenous production is directly related to its elusive nature and the difficulties surrounding unequivocal and quantitative detection, especially when NO is present.

In the past decade several methods^{16–23} have been developed allowing detection and quantification of azanone with discrimination from NO and other reactive nitrogen and oxygen species, RNOS. These methods include chemical trapping and HPLC product characterization,¹⁷ UV-vis,^{19–21} and fluorescence^{22,24–26} detection and electrochemical detection.^{27–29} In particular, our group has developed both a UV-vis trapping-based detection method that uses manganese porphyrins (MnP) and an azanone sensing electrode that is able to provide time-resolved quantification of HNO at the low nanomolar level.^{21,28}

In a broader sense, the biological relevance of nitroxyl has at least two important aspects. The first concerns the studies of the pharmacological effects of HNO and the elucidation of the similarities with and the differences from NO.^{30–34} The second is related to the possibility of its endogenous production as a biologically relevant messenger,³¹ an intermediate metabolite,^{35–38} or an undesired enzymatic side product.^{35–38} In this context,

Received: December 10, 2014

several *in vivo* azanone sources have been proposed. For example, HNO production could result from the activity of nitric oxide synthase (NOS) in the absence of the redox cofactor tetrahydrobiopterin.^{36,38–41} Another well established *in vitro* enzymatic azanone source relies on the oxidation of hydroxylamine and other amino alcohols. Several groups have shown that this reaction can be catalyzed by heme-proteins like peroxidases, catalases, or even myoglobin.^{17,42} On the other hand, chemical (nonenzymatic), biologically compatible routes to HNO have been, to our knowledge, much less pursued.^{31,43} The most direct route, chemical reduction of NO, has been historically discarded, possibly due to the reduction potential of -0.8 V for the (NO/³NO⁻) couple, which is outside the biological range. However, at physiological pH, ¹HNO is expected to be the main species ($\text{p}K_{\text{a}} = 11.4$),⁹ displaying an estimated E° (NO, H⁺/¹HNO) ≈ -0.14 V.^{9,44} Moreover, it is important to note that the reduction of NO to HNO (reaction 1) could be driven forward by coupling with subsequent thermodynamically favorable reactions, such as N₂O production (reaction 2) or reactions between radical intermediates (reaction 3).



Interestingly, our recent results showed that HNO can be produced *in vivo* by the reaction of NO⁵ or the nitrosyl species^{30,45,46} with H₂S ($E^{\circ}(\text{S}^{\bullet-}, 2\text{H}^{+}/\text{H}_2\text{S}) = E^{\circ}(\text{S}^{\bullet-}, \text{H}^{+}/\text{HS}^{-}) = 0.92$ V at pH 7).⁴⁵ Also noteworthy, are several older works which showed that NO rebinds with generated H[•] to yield azanone.^{47–50} In this work we demonstrate that NO can actually be reduced to azanone by several biologically relevant compounds bearing the $-\text{OH}$ functional group resulting in a novel potential pathway for endogenous production of HNO.

EXPERIMENTAL SECTION

Reagents. Mn(III) 5,10,15,20-tetrakis(4-carboxyphenyl)-porphyrinate was purchased from Frontier Scientific and used as received. All reagents were purchased from Sigma-Aldrich and used as received. Trioxodinitrate (N₂O₃²⁻) was synthesized according to published literature procedures.^{29,51,52} Milli-Q grade water was used in all experiments; nitrogen and argon of high purity were used for anaerobic experiments. NO was generated anaerobically by dropwise addition of degassed water to a mixture of 4 g of NaNO₂, 8.5 g of FeSO₄, and 8.5 g of NaBr. The so-produced NO was passed through a NaOH solution to remove higher oxides and bubbled into degassed water in order to get a saturated solution of NO ([NO] = 2 mM).

Optical Absorbance. Measurements were recorded using an HP8453 spectrophotometer in 1 cm path-length quartz cuvette and using as blank the respective buffer solutions. All experiments were performed at 25 °C in 0.1 M phosphate buffer, pH 7.4, containing DPTA 10⁻⁴ M to avoid interferences or undesired reactions by Cu^{II} or other divalent cations. We also checked that all reactions were unaffected by the irradiation of the sample with the light source of the spectrometer.

Infrared Spectrometry. Spectra from 400 to 4000 cm⁻¹ with 1 cm⁻¹ resolution were recorded with a research series Thermo Nicolet FTIR spectrophotometer. All gas phase IR spectra were recorded using an 8 cm path length gas cell with NaCl windows. The IR spectrum of the N₂O present was quantified using calibration curves for the absorption bands showing peaks at 2212 and 2236 cm⁻¹ for the P and R branches, respectively.⁵³ Under these conditions nitrous oxide signals for each injection were compared to a calibration curve

prepared by injecting samples of N₂O produced *in situ* by NO₂⁻ BSHA decomposition.²⁹ The detection limit for N₂O in the present conditions was 0.5 μmoles.

Amperometry. Measurements of HNO concentration were carried out with our previously described method based on a three-electrode system consisting of platinum counter electrode, Ag/AgCl reference electrode, and a gold working electrode modified with a monolayer of cobalt porphyrin with 1-decanethiol covalently attached. The method has been demonstrated to be specific for HNO, showing no interference or spurious signal due to the presence of NO, O₂, NO₂⁻, and other RNOS.^{27,28,53} Signal recording was performed with a TEQ 03 potentiostat.

In a typical experiment, 1.2 to 24 pmoles of ROH (0.2 to 4 μM) were added to 1.2 μmoles of NO dissolved in 6 mL (0.2 mM) of degassed distilled water containing 0.6 μmoles of DPTA (or EDTA) at room temperature (r.t.) under Ar atmosphere (or vice versa). For each case, we also confirmed that the maximum used concentrations (0.2 mM) of NO, and all H[•] donors produced a very small signal that can be disregarded. We have also performed the reaction of NO with AscH⁻ in an oxygen-free glovebox. In this case, water was deoxygenated by distillation under nitrogen atmosphere after addition of sodium dithionite. The results were very similar to those obtained with degassed water (Supporting Information, Figure S13B).

Ion Chromatography. Measurements were recorded using a DIODEX DX-100 system, with an AS4A-SC (4 mm × 250 mm) column and an AG4A-SC guard column. The carrier was CO₃²⁻/HCO₃⁻ 1.8/1.7 mM, with a flow rate of 2 mL/min

EPR Measurements. Solutions and buffers were prepared using high purity reagents and milli-Q grade water. All glassware was previously washed with HNO₃ and abundant milli-Q water and silicone tubing and plastic syringes were used to transfer solutions. Diethylene triamine pentaacetic acid (DTPA) (0.5 mM) and/or ethylene diamine tetraacetic acid (EDTA) (8 mM) were used as chelating agents to remove possible traces of catalytic metal ions. O₂ was eliminated from all solutions through vacuum-Ar cycles and a positive Ar pressure was maintained by bubbling Ar gas on the solutions throughout all handling.

For ascorbate anion, time scan experiments at a fixed magnetic field were also performed. The field B₀ was chosen as the maximum of the low-field peak corresponding to the ascorbyl radical anion doublet. These experiments were performed with 1 G modulation amplitude, 6.33 mW microwave power, and a conversion time of 20 ms.

Computational Methods. To determine the reaction mechanism we performed DFT calculations using the Gaussian 98 software package. All involved species were optimized at the B3LYP level using 6-31 G(d,p) for all atoms using water (polarizable continuum model-PCM) in order to take into account solvation effects.

Mass Spectrometry. MS experiments were performed on maXis (Bruker Daltonics) ultrahigh resolution electron spray ionization time-of-flight mass spectrometer equipped with cryospray ionization module (Bruker Daltonics). Into 100 μM ascorbate solution in 80% acetonitrile/20% 10 mM ammonium carbonate buffer pH 7.4, 500 μM NO was added, and the reaction mixture was sprayed at -20 °C. Spectra were recorded over 15 min time.

Cell Experiments. Bovine Aorta Endothelial cell (BAEC, CLS Cell Lines Service GmbH, Germany) were grown in Ham's F12 medium supplemented with 2 mM L-glutamine and 10% fetal bovine serum at 37 °C and 5% CO₂. Cells were loaded with CuBOT1 and fluorescence was recorded as previously described.^{25,45} RAW 264.7 (mouse monocyte macrophage) from ECACC (Salisbury, UK) were grown in DMEM (Sigma-Aldrich, USA, cat. no. D5546) cell medium supplemented with 2 mM L-glutamine (Sigma-Aldrich, USA), 10% FBS (Sigma-Aldrich, USA), 1% penicillin-streptomycin (Sigma-Aldrich, USA), and 1% nonessential amino acid solution (Sigma-Aldrich, USA) in T-75 cell culture flask at 5% CO₂ and at 37 °C. Cells were stimulated with 1 μg/mL LPS (Sigma-Aldrich, USA) overnight and next day mechanically detached, washed once with HBSS with Ca²⁺ and Mg²⁺, and used immediately for analysis. We used 1 × 10⁶ cells per sample in HBSS with Ca²⁺ and Mg²⁺ supplemented with different concentration of FBS (fetal bovine serum) up to 5%. The

198 temperature of the HBSS w/o Ca^{2+} and Mg^{2+} used in measurement
199 experiments was 37 °C.

200 ■ RESULTS AND DISCUSSION

201 **Aromatic Alcohols and Ascorbate React with NO to**
202 **Produce HNO.** Our first approach to determine the possible
203 production of HNO from the reaction of NO with aliphatic or
204 aromatic alcohols was performed by measuring the conversion
205 of Mn(III)TCPP to $\{\text{MnNO}\}^6$ (Enemark-Feltham notation)
206 using UV-vis spectroscopy (see Supporting Information for
207 more details).⁵⁴ Figure S11A shows the absorbance changes
208 obtained after mixing NO solution with ascorbate (AscH^-),
209 the predominant species under the reaction conditions. These
210 changes are characteristic for the reaction between Mn(III)
211 porphyrins and HNO, with the consequent formation of
212 $\{\text{MnNO}\}^6$.²¹ Since this Mn(III) porphyrin reacts neither with
213 NO^{21} nor with ascorbate⁵⁵ (see control experiments in
214 Supporting Information, Figure S11 and S12) these results
215 strongly suggest HNO production. Similar results were
216 obtained with hydroquinone (HQ), tyrosine (Y), and phenol
217 (PhOH), although the reaction rates varied significantly (see
218 Table 1). No reaction was observed with nonaromatic alcohols

Table 1. Amounts of N_2O and Nitrite Obtained for the Reactions of H^\bullet Donors with NO, and the Corresponding k_{eff}

compound ^a	k_{eff} ($\text{M}^{-1} \text{s}^{-1}$) ^b	NO_2^- (μmol) ^c	N_2O (μmol) ^c	N_2O yield ^c	org. prod. yield ^d
AscH ⁻	8.0 ± 0.5 (43 ± 15)	20	16	50%	>95%
HQ	6.1 ± 0.4 (9)	11	9	30%	>95%
PhOH	3.2 ± 0.4	8	6	20%	~ 90%
Y	0.9 ± 0.4	5	4	10%	~ 30%

^aNo reaction was detected when methanol, D-mannitol or malic acid were used. ^bDetermined from the slope of the electrode signal. Between parentheses, determined by EPR, see Supporting Information for details. ^cAfter 24 h, based on the initial amount of NO (100 μmol). ^dDehydroascorbate (DHA), benzoquinone (BQ), *p*-Ph(OH)-NO, and *o*-Y-NO respectively, based on 17 μmol (initial amount).

219 like methanol, D-mannitol, or malic acid. The second approach
220 used to determine HNO production relied on the recently
221 developed HNO selective electrode, which allows time-resolved
222 nanomolar detection.^{27–29,53} In Figure 1 we present the
223 amperometric signal versus initial time plot after the addition
224 of each alcohol (2 μM) to an anaerobic aqueous solution of
225 NO (0.2 mM). The increase in the current following the
226 addition of the alcohol clearly proves the HNO formation. As
227 expected for a bimolecular reaction, the signal peak, which
228 reflects the HNO concentration,²⁸ is linearly dependent on
229 both AscH^- and NO concentrations (Supporting Information,
230 Figure S13).

231 Figure 2A and Supporting Information, Figure S13C show
232 that v_i (initial rate) versus $[\text{ROH}]$ and $[\text{NO}]$ plots are linear.
233 From the slope of these plots an effective bimolecular reaction
234 rate constant (k_{eff}), corresponding to reaction 1 can be
235 obtained.

$$v = k_{\text{eff}}[\text{ROH}][\text{NO}]$$

236 The resulting k_{eff} are reported in Table 1, and the data show
237 that both diols (HQ and AscH^-) react ca. 5–10 times faster
238 than phenols, with AscH^- being the fastest.

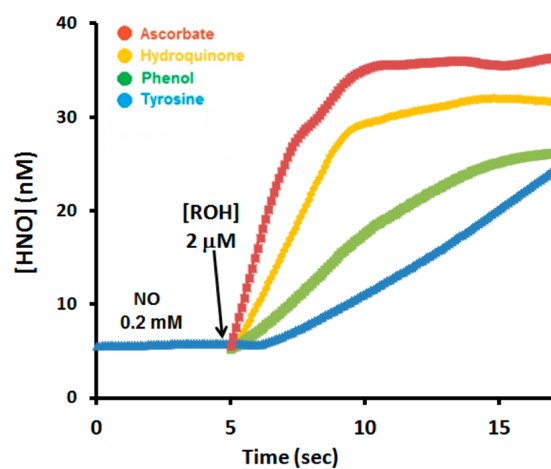


Figure 1. Amperometric signal vs initial time plot after the addition of 2 μM ROH to an anaerobic aqueous solution of NO (0.2 mM): y-axis, $[\text{HNO}]$ after calibration. ROH = (red) AscH^- ; (orange) HQ; (green) PhOH; (blue) Y.

239 On the other hand, Figure 2B and Supporting Information, 239
240 Figure S13D show that the $\log(v_i)$ vs $\log[\text{ROH}]$ and $\log[\text{NO}]$ 240
241 plots are linear with a slope close to 1, confirming that the 241
242 reaction is first order in both reactants. 242

243 We also tested whether Fe(II/III), Mn(II), Cu(I/II), or 243
244 Co(II) affected HNO production in the described reactions by 244
245 using the electrochemical nitroxyl sensor. The results confirmed 245
246 that metal ions do not play any significant role in the 246
247 production of HNO (see Supporting Information, Table S12). 247

248 **EPR Analysis.** Since a formal H atom abstraction from 248
249 $-\text{OH}$ groups by NO would produce a free radical species, the 249
250 reactions were studied by EPR. Ascorbate (0.2–2 mM), 250
251 hydroquinone (10 mM), and tyrosine (2 mM) solutions were 251
252 mixed with equal volumes of the NO saturated solutions by 252
253 simultaneous rapid injection into a quartz flat cell. The 253
254 presence of dioxygen and metal ions (DPTA or EDTA were 254
255 used as chelators) was excluded. The first two alcohols 255
256 produced clearly detectable EPR signals as shown in Figure 3 256
257 and Supporting Information, Figure S15. Tyrosyl radicals were 257
258 not observed, presumably due to the slower reaction rate 258
259 between NO and Y and/or the lower stability of the tyrosyl 259
260 radical. Figure 3 shows the time dependence of the ascorbyl 260
261 radical concentration obtained after mixing AscH^- and NO. 261

262 After mixing the reactants, an intense ascorbyl radical signal 262
263 appears which subsequently decays with a half-life of 4–8 s. 263
264 This behavior is consistent with disproportionation of the 264
265 ascorbyl radical into ascorbate and dehydroascorbate,⁵⁶ and 265
266 also reaction of ascorbyl with NO to give O-nitrosoascor- 266
267 bate.^{43,57} For the reaction with HQ (shown in Supporting 267
268 Information, Figure S15) similar results were obtained, but the 268
269 radical signal corresponding to HQ^\bullet increases 6-fold and 269
270 remains stable for several minutes, slightly decaying after 15 270
271 min. The EPR signals also allow determination of the k_{eff} for 271
272 both reactions (shown in Table 1). k_{eff} values obtained by EPR 272
273 are in the same order of magnitude as those obtained from the 273
274 electrochemical data. 274

275 The ubisemiquinone EPR signal has been reported during 275
276 the reaction between NO and truncated ubiquinols,⁵⁸ and the 276
277 ascorbyl radical has been observed during the reaction between 277
278 ascorbate and N-acetyl-N-nitrosotryptophan or NO donors 278
279 under normoxic and oxygen free conditions.⁴³ The kinetic 279

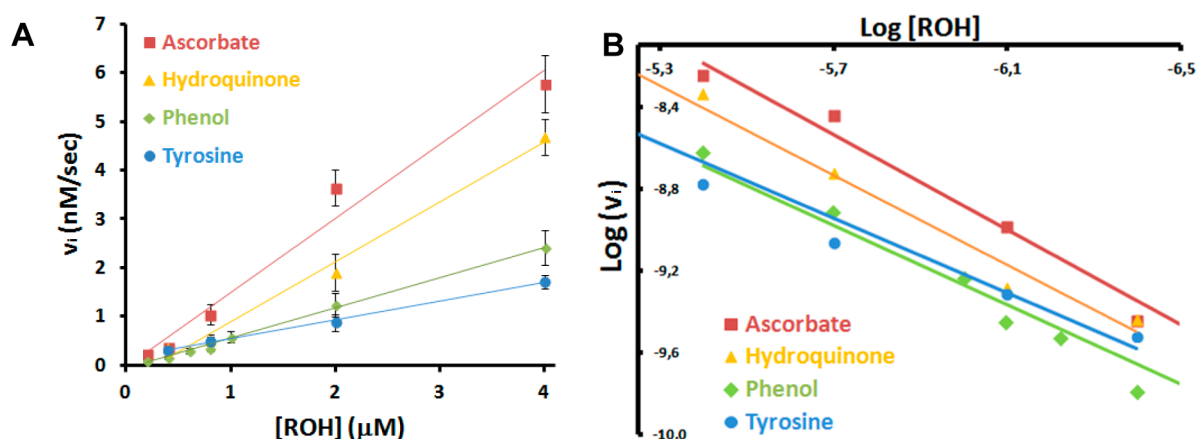


Figure 2. (A) v_i vs $[ROH]$. (B) $\log(v_i)$ vs $\log[ROH]$. $[NO] = 0.2$ mM. ROH = (red) AsC $^{\bullet-}$; (orange) HQ; (green) PhOH; (blue) Y.

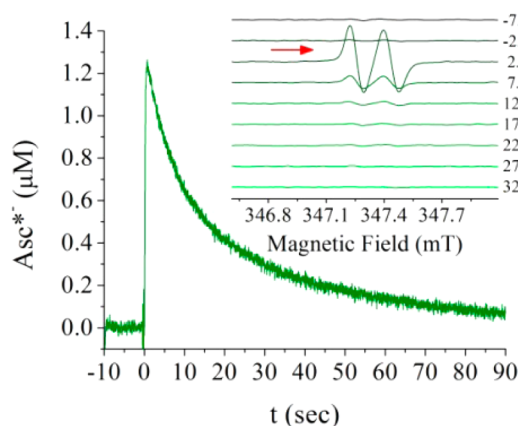


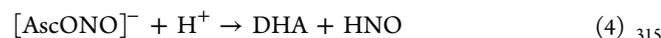
Figure 3. Time dependence of ascorbyl radical concentration. Inset: Consecutive EPR spectra of solutions of ascorbate (1 mM) alone and with NO (1 mM). The arrow indicates beginning of the reaction.

280 analysis of these reactions is detailed in the Supporting
281 Information.

282 **End Products Analysis.** The initial products of the
283 reaction of NO with the alcohols are unstable and highly
284 reactive radical species. Thus, further reactions are expected to
285 occur. The main sink for HNO is expected to be its
286 dimerization and/or reaction with NO,¹⁰ yielding the stable
287 products N₂O and NO₂⁻. To detect and quantify N₂O we
288 determined the IR spectra of the reaction chamber headspace.
289 As expected, NO reaction with HQ, AsC $^{\bullet-}$, Y, and PhOH
290 results in the appearance of characteristic N₂O IR bands at
291 2210 and 2230 cm⁻¹ (see Supporting Information, Figure
292 SI7),^{53,59} and no signal is observed with either reactant alone.
293 The presence of nitrite was confirmed by ion chromatography
294 (see Figure SI8). Moreover, quantification of the relative N₂O
295 and NO₂⁻ yields (Table 1) show that they are formed in a ca.
296 1:1 ratio, which is consistent with our mechanistic interpreta-
297 tion (eq 9; vide infra).

298 The R-O $^{\bullet}$ radicals are also inherently unstable and thus react
299 further leading to more stable organic closed shell compounds.
300 To determine the corresponding end products for each
301 reaction, we used NMR spectroscopy, IR, UV, and MS
302 spectrometry (see Supporting Information). AsC $^{\bullet-}$ yields
303 dehydroascorbate (DHA) as the main end product, formed
304 by ascorbyl radical disproportionation. When studied by cryo-
305 spray ionization ultrahigh-resolution mass spectrometry, the
306 reaction of AsC $^{\bullet-}$ and NO showed MS peaks (m/z 207.0368,

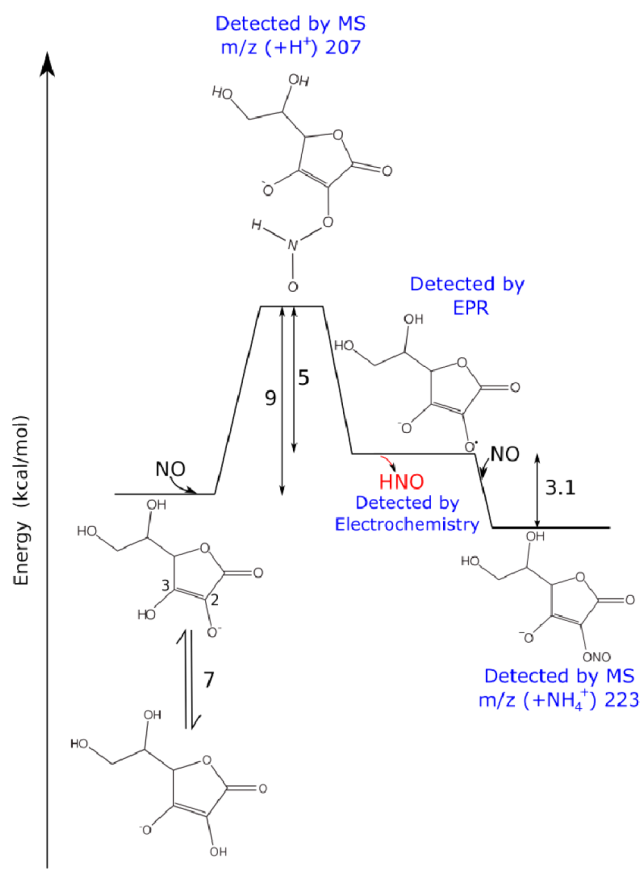
223.0591 and 237.0378, Supporting Information, Figure SI9),
307 which correspond to the first addition of NO to ascorbate, and
308 second addition of NO to either first RO-NO $^{\bullet-}$, or the ascorbyl
309 radical (see below for mechanistic analysis). As postulated by
310 Kirsch,⁴³ once the nitrite ester [AscONO] $^{\bullet-}$ is formed by the
311 reaction of AsC $^{\bullet-}$ with NO, HNO and DHA can be produced
312 via a radical chain mechanism as shown in eq 4,⁴³ eq 5,⁶⁰ and eq
313 6.⁴³ 314



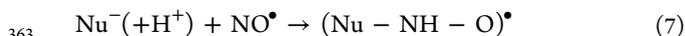
HQ yields mainly benzoquinone (BQ), also possibly due to
318 further reaction of the HQ radical with NO. Finally, PhOH and
319 Y yield the corresponding products 4-nitrosophenol (*p*-
320 Ph(OH)-NO) and 3-nitrosotyrosine (*o*-Y-NO), whereas Y
321 also dimerizes to yield dityrosine (see Supporting Information
322 for experimental details); these products are consistent with the
323 presence of PhO $^{\bullet}$ and Y $^{\bullet}$ radicals. The lack of EPR signal in
324 these cases possibly arises because of their high reactivity and
325 the presence of the excess of NO, which yields the mentioned
326 products. The yields of the organic products (see Supporting
327 Information for details) are higher than the corresponding N₂O
328 yields, indicating that these compounds are also produced by
329 other routes which do not afford HNO. The formation of
330 nitrosocompounds by reaction of phenols with NO has been
331 observed before.⁶¹ 332

Computational Mechanistic Analysis. To get an addi-
333 tional insight into the reaction mechanisms we performed DFT
334 calculations using the Gaussian software package. As an
335 example, the results for AsC $^{\bullet-}$ are presented in Scheme 1,
336 while the other cases are shown in Supporting Information,
337 Figure SI11. The calculations show that the first step of the
338 reaction between NO and AsC $^{\bullet-}$ is endergonic (by 16 kcal/
339 mol) yielding a radical intermediate RO-N(H)O $^{\bullet}$ (consistent
340 with one of the peaks observed in the mass spectrometer at m/z
341 207.0368, see Scheme 1 and Supporting Information, Figure
342 SI9). This step can be described as a nucleophilic attack of the
343 ascorbate anion to NO (reaction 7), coupled to proton transfer
344 from the vicinal -OH moiety or the solvent. Such a mechanism
345 can be described as a proton-coupled nucleophilic attack
346 (PCNA). 347

NO binds preferably to C2-O, while ascorbate is preferably
348 deprotonated at C3-O (see Scheme 1). At this point it is 349

Scheme 1. DFT Calculations. Energy Values Reported in kcal/mol

350 difficult to determine whether the NO reacts with one or the
 351 other tautomer, with the OH or O⁻, and how and when the
 352 protons are transferred. However, attack of -O⁻ to NO seems to
 353 be more likely. The RO-N(H)O[•] radical intermediate decays
 354 to HNO and the ascorbyl radical (reaction 8), which can then
 355 react with another NO to produce a closed shell nitrite ester *o*-
 356 nitrosoascorbate (also observed by MS at *m/z* 223.0591).
 357 Reaction of the radical with the second NO prior to its HNO
 358 release, possibly accounts for formation of di-ONO observed by
 359 MS (*m/z* 237.0378, Supporting Information, Figure S19g). The
 360 *O*-nitrosoascorbate also decays after taking a proton to yield
 361 HNO and DHA, as previously observed by Kirsch and co-
 362 workers.⁵⁷



365 A similar mechanism is expected for HQ (see Supporting
 366 Information), with two NO molecules reacting with each HQ
 367 molecule. For Y and PhOH, the radical intermediates produced
 368 after the addition of NO, formation of the RO-N(H)O
 369 intermediate, and HNO release also yield the observed nitroso
 370 derivatives. More importantly, taking into account the p*K*_a of
 371 the corresponding alcohol, in these three cases the reaction
 372 undoubtedly occurs with a neutral OH group, where an
 373 intramolecular proton rearrangement or solvent-assisted
 374 protonation is required. Therefore, in these cases a PCNA is
 375 proposed as well.

376 Last but not least, it is important to note that although the
 377 first reaction step between NO and alcohol is endergonic, the

reaction is driven forward by the subsequent reactions of the
 378 initial products (HNO and radicals). In fact, HNO dimerization
 379 overcompensates the endergonic HNO generation resulting in
 380 an overall negative free energy balance for the global reaction 9
 381 (see Scheme 1), which for AscH⁻ is
 382



The energy associated with the first step, either to yield directly
 384 HNO by HAT or an “RON(H)O–like” radical intermediate by
 385 PCNA, can be considered a minimum estimation of the global
 386 reaction barrier. As shown in Table 2, the Δ*E* for the first two
 387 12

Table 2. Ab Initio Calculated Reaction Energies (Δ*E*) in kcal/mol for PCNA and HNO Release Steps

	p <i>K</i> _a	<i>E</i> ^o (V) (pH 7) RO [•] / H ⁺ /ROH	Δ <i>E</i> PCNA ^a	Δ <i>E</i> HNO release ^a	Δ <i>E</i> step 1+2 ^a	global ^{a,c}
AscH ⁻	4.11	0.28	+16	- 5	+11	-58
HQ	10	0.10	+ 18.5	10.5	+ 8	-109
Y	10	0.91	+ 25.4	+ 7.4	+33	-63
PhOH	10	0.97	+25.3	+12.4	+37.7	-70
MeOH ^b	15.5	-	+ 19.5	+ 33.7	+53.2	-

^aΔ*E*_{PCM} (kcal/mol), optimized at the B3LYP level using 6-31 G(d,p) for all atoms using water (PCM: polarizable continuum model); step 1, PCNA; step 2, HNO release. ^bHNO was not detected when methanol was used. ^cFinal product was DHA, BQ, *p*-Ph(OH)NO, and *o*-YNO, respectively (see SI).

steps (step 1+2) are smaller for AscH⁻ and HQ, which are the
 388 faster reactants (Table 1). The largest Δ*E* (+53.2 kcal/mol) is
 389 observed for MeOH, which does not react under the tested
 390 conditions. The calculated energies for step 1+2 and for the
 391 global reaction are in reasonable agreement with those energies
 392 obtained from tabulated redox potentials (Supporting In-
 393 formation, Table S13).
 394

To assess the potential role of molecular oxygen on these
 395 reactions, we performed the reaction of AscH⁻ and NO in the
 396 presence of controlled amounts of oxygen (Supporting
 397 Information, Figures S12 and S14). As shown in Figure S14,
 398 the amount of HNO produced decreases as the relative amount
 399 of added O₂ is increased. This is a strong indication that O₂
 400 does not catalyze HNO formation. Instead, the presence of O₂
 401 diminishes the observed signal, a fact that can be attributed to
 402 its known reaction with either reactant, or even with azanone,
 403 as shown in our previous work.²⁸
 404

In Vitro Cell Studies. In certain cell types, such as
 405 endothelial cells, neuronal cells, and immune cells, vitamin C
 406 accumulates to concentrations higher than 1 mM.⁶² To analyze
 407 whether the described reactions occur under physiological
 408 conditions, we used an HNO fluorescence sensor, CuBOT1, to
 409 evaluate the intracellular azanone formation.^{22,24–26} Bovine
 410 arterial endothelial cells were pretreated with either 1 mM
 411 AscH⁻ or 1 mM pBQH2 for 1 h to increase their intracellular
 412 concentration. Cells were washed and then loaded with
 413 CuBOT1 to assess the changes in intracellular levels of
 414 HNO. The intensity of the fluorescence was compared with
 415 basal fluorescence detected in the control (untreated cells).
 416 Figure 4A shows a clear increase of the fluorescence with both
 417 14 treatments. In addition we tested the ability of ascorbate to
 418 reduce endogenously generated NO from another cell line,
 419 RAW 264.7 macrophages. Macrophages were stimulated with
 420 lipopolysaccharide(LPS)/interferon gamma to stimulate indu-
 421

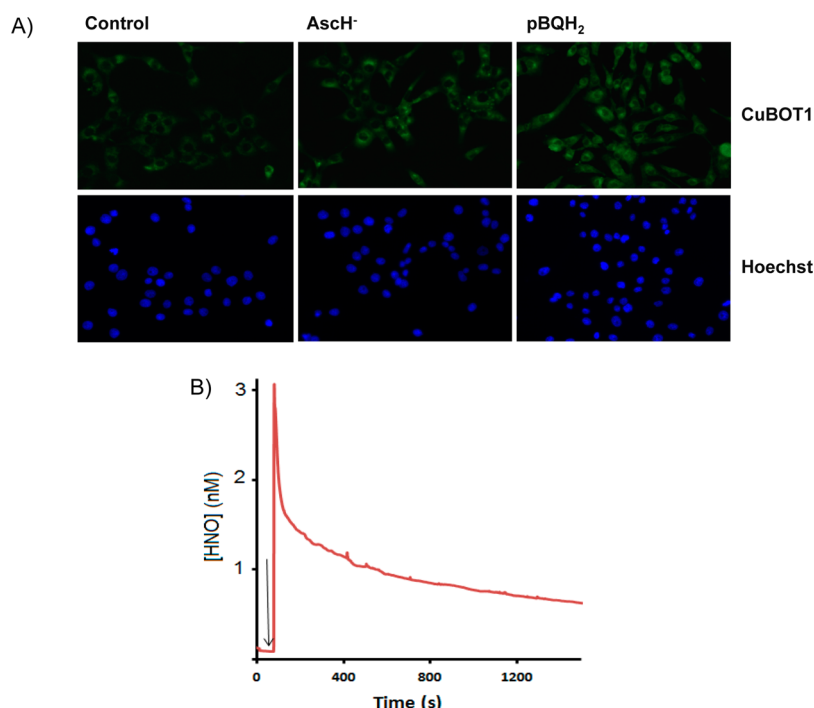


Figure 4. (A) Intracellular HNO formation in bovine arterial endothelial cells as revealed by the HNO fluorescence sensor, CuBOT1. Hoechst was used to stain the nuclei, showing that there are cells in the control for which the signal is very low, and also that the position of the signal matches the actual cells. (B) HNO formation after the addition of ascorbate to immunostimulated macrophages. The HNO electrode was immersed into a 10^6 cell/mL suspension of immunostimulated macrophages in Dulbecco's Modified Eagle's Medium (DMEM). Subsequently 1 mM ascorbate was added, and the current was monitored.

422 cible nitric oxide synthase to produce NO, and the HNO
423 electrode was immersed in the extracellular medium containing
424 10^6 cells/mL. After the addition of 1 mM ascorbate an
425 immediate rise in the signal was observed, showing clear HNO
426 formation (Figure 4B). No signal was observed when AscH^-
427 was added into cell-free medium.

428 These data strongly suggest that HNO could be produced in
429 the reaction of NO and AscH^- under physiological conditions.

430 CONCLUSIONS

431 The present work provides clear evidence of a possible
432 biochemically relevant HNO source, resulting from the reaction
433 of NO with aromatic or "pseudoaromatic" alcohols such as
434 tyrosine, ascorbic acid, and hydroquinone. Mechanistically, it is
435 clear that the reaction does not involve a simple outer sphere
436 reduction coupled to proton release/uptake, which is
437 thermodynamically unfavorable as evidenced by the alcohol
438 reduction potentials shown in Table 2.

439 Instead, our data suggest that there is a nucleophilic addition
440 of ROH/RO^- to NO, coupled to a proton transfer (either
441 intramolecular or through the solvent) that results in an RO-
442 N(H)O^\bullet intermediate, which decays by O–N bond cleavage,
443 producing HNO and the corresponding radical (see Scheme 2
444 and Table 2). The stability of the RO^\bullet radical (bound to HNO

or free), PCNA endergonicity, and the global energy for steps 1
+ 2 (Table 2) seems to be the key factor for the reaction to
occur, explaining why no reaction is observed for MeOH or
mannitol, and why AscH^- and HQ react faster.

Beyond the chemical novelty, biological implications are
direct. For example, given the known preference for NO
partition within the hydrophobic interior of biological
membranes⁶³ and its physiological role in plant and animal
mitochondria, the following picture emerges:^{64,65} under
hypoxia, respiratory chain intermediate quinones accumulate
and NO production increases, through nitrite reductase activity
of myoglobin among others,⁶⁶ creating an ideal opportunity for
the presented reaction to take place. In addition, the presented
proof of concept for physiological NO conversion to HNO,
suggests that it is not unlikely that some of the protective
effects assigned to NO, are indeed mediated by its "younger"
sibling HNO,⁶⁷ as shown in our recent work.³¹

Definitive proof to these hypotheses awaits further studies
and opens the way for both potential therapeutic interventions
of azanone donors and understanding of endogenous HNO
production.

ASSOCIATED CONTENT

Supporting Information

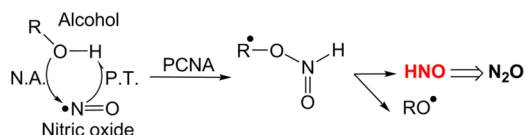
Kinetic analysis, ab initio calculations, mass spectra, EPR, and
other experimental details. This material is available free of
charge via the Internet at <http://pubs.acs.org>.

AUTHOR INFORMATION

Corresponding Authors

doctorovich@qi.fcen.uba.ar
marcelo@qi.fcen.uba.ar

Scheme 2. Proposed Mechanism for HNO Formation by the Reaction of NO with ROH



475 **Notes**

476 The authors declare no competing financial interest.

477 **ACKNOWLEDGMENTS**

478 This work was financially supported by UBA (UBACYT W583
479 and 2010-12), ANPCyT (PICT 2010-2649 and 2010-416),
480 CONICET (PIP1207 and 112-201001-00125), and from the
481 Bunge y Born Foundation. S.A.S. and L.A. thank CONICET for
482 a fellowship grant, NIN, DEB, CDB, MAM, and FAD are
483 members of CONICET. J.M., M.R.F., and I.I.-B acknowledge
484 the support by intramural funds provided by the FAU within
485 the Emerging Field Initiative (Medicinal Redox Inorganic
486 Chemistry).

487 **REFERENCES**

- 488 (1) Napoli, C.; Paolisso, G.; Casamassimi, A.; Al-Omran, M.;
489 Barbieri, M.; Sommese, L.; Infante, T.; Ignarro, L. J. *J. Am. Coll.*
490 *Cardiol.* **2013**, *62*, 89.
491 (2) Tonzetich, Z. J.; McQuade, L. E.; Lippard, S. J. *Inorg. Chem.*
492 **2010**, *49*, 6338.
493 (3) Goodrich, L. E.; Paulat, F.; Praneeth, V. K. K.; Lehnert, N.;
494 Arbor, A. *Biochemistry* **2010**, *49*, 6293.
495 (4) Martínez-Ruiz, A.; Cadenas, S.; Lamas, S. *Free Radic. Biol. Med.*
496 **2011**, *51*, 17.
497 (5) Bruce King, S. *Free Radic. Biol. Med.* **2013**, *55*, 1.
498 (6) Irvine, J. C.; Ritchie, R. H.; Favaloro, J. L.; Andrews, K. L.;
499 Widdop, R. E.; Kemp-Harper, B. K. *Trends Pharmacol. Sci.* **2008**, *29*,
500 601.
501 (7) Flores-Santana, W.; Salmon, D. J.; Donzelli, S.; Switzer, C. H.;
502 Basudhar, D.; Ridnour, L.; Cheng, R.; Glynn, S. A.; Paolucci, N.;
503 Fukuto, J. M.; Miranda, K. M.; Wink, D. A. *Antioxid. Redox Signal.*
504 **2011**, *14*, 1659.
505 (8) Miranda, K. M. *Coord. Chem. Rev.* **2005**, *249*, 433.
506 (9) Shafirovich, V.; Lyman, S. V. *Proc. Natl. Acad. Sci. U.S.A.* **2002**, *99*,
507 7340.
508 (10) Lyman, S. V.; Shafirovich, V.; Poskrebyshev, G. A. *Inorg. Chem.*
509 **2005**, *44*, 5212.
510 (11) Miranda, K. M.; Nims, R. W.; Thomas, D. D.; Espey, M. G.;
511 Citrin, D.; Bartberger, M. D.; Paolucci, N.; Fukuto, J. M.; Feelisch, M.;
512 Wink, D. A. *J. Inorg. Biochem.* **2003**, *93*, 52.
513 (12) Liochev, S. *Free Radic. Biol. Med.* **2003**, *34*, 1399.
514 (13) Bartberger, M. D.; Fukuto, J. M.; Houk, K. N. *Proc. Natl. Acad.*
515 *Sci. U.S.A.* **2001**, *98*, 2194.
516 (14) Ford, P. C. *Inorg. Chem.* **2010**, *49*, 6226.
517 (15) Hoshino, M.; Laverman, L.; Ford, P. C. *Coord. Chem. Rev.* **1999**,
518 *187*, 75.
519 (16) Cline, M. R.; Tu, C.; Silverman, D. N.; Toscano, J. P. *Free Radic.*
520 *Biol. Med.* **2011**, *50*, 1274.
521 (17) Reisz, J. A.; Zink, C. N.; King, S. B. *J. Am. Chem. Soc.* **2011**, *133*,
522 11675.
523 (18) Donzelli, S.; Espey, M. G.; Flores-Santana, W.; Switzer, C. H.;
524 Yeh, G. C.; Huang, J.; Stuehr, D. J.; King, S. B.; Miranda, K. M.; Wink,
525 D. A. *Free Radic. Biol. Med.* **2008**, *45*, 578.
526 (19) Suárez, S. A.; Martí, M. A.; De Biase, P. M.; Estrin, D. a.; Bari, S.
527 E.; Doctorovich, F. *Polyhedron* **2007**, *26*, 4673.
528 (20) Dobmeier, K. P.; Riccio, D. A.; Schoenfish, M. H. *Anal. Chem.*
529 **2008**, *80*, 1247.
530 (21) Martí, M. A.; Bari, S. E.; Estrin, D. A.; Doctorovich, F. *J. Am.*
531 *Chem. Soc.* **2005**, *127*, 4680.
532 (22) Zhou, Y.; Liu, K.; Li, J.-Y.; Fang, Y.; Zhao, T.-C.; Yao, C. *Org.*
533 *Lett.* **2011**, *13*, 2357.
534 (23) Doctorovich, F.; Bikiel, D.; Pellegrino, J.; Suárez, S. A.; Larsen,
535 A.; Martí, M. A. *Coord. Chem. Rev.* **2011**, *255*, 2764.
536 (24) Tennyson, A. G.; Do, L.; Smith, R. C.; Lippard, S. J. *Nitric Oxide*
537 **2006**, *26*, 1.
538 (25) Rosenthal, J.; Lippard, S. J. *J. Am. Chem. Soc.* **2010**, *132*, 5536.

- (26) Wrobel, A. T.; Johnstone, T. C.; Liang, A. D.; Lippard, S. J.; 539
Rivera-fuentes, P. *J. Am. Chem. Soc.* **2014**, *136*, 4697. 540
(27) Suárez, S. A.; Fonticelli, M. H.; Rubert, A. A.; de la Llave, E.; 541
Scherlis, D.; Salvarezza, R. C.; Martí, M. A.; Doctorovich, F. *Inorg.* 542
Chem. **2010**, *49*, 6955. 543
(28) Suárez, S.; Bikiel, D.; Wetzler, D.; Martí, M. A.; Doctorovich, F. 544
Anal. Chem. **2013**, *85*, 10262–10269. 545
(29) Sirsalmath, K.; Suárez, S. A.; Bikiel, D. E.; Doctorovich, F. *J.* 546
Inorg. Biochem. **2013**, *118*, 134. 547
(30) Filipovic, M. R.; Eberhardt, M.; Prokopovic, V.; Mijuskovic, A.; 548
Orescanin-Dusic, Z.; Reeh, P.; Ivanovic-Burmazovic, I. *J. Med. Chem.* 549
2013, *56*, 1499. 550
(31) Eberhardt, M.; Dux, M.; Namer, B.; Miljkovic, J.; Cordasic, N.; 551
Will, C.; Kichko, T. I.; Roche, J.; de la Fischer, M.; Bikiel, D.; Suárez, S. 552
A.; Dorsch, K.; Leffler, A.; Babes, A.; Lampert, A.; Lennerz, J. K.; 553
Jacobi, J.; Martí, M. A.; Doctorovich, F.; Högestätt, E. D.; Zygmunt, P. 554
M.; Ivanovic-Burmazovic, I.; Messlinger, K.; Reeh, P.; Filipovic, M. R. 555
Nat. Commun. **2014**, *5*, 4381. 556
(32) Fukuto, J. M.; Cisneros, C. J.; Kinkade, R. L. *J. Inorg. Biochem.* 557
2013, *118*, 201. 558
(33) Miranda, K. M.; Paolucci, N.; Katori, T.; Thomas, D. D.; Ford, 559
E.; Bartberger, M. D.; Espey, M. G.; Kass, D. a; Feelisch, M.; Fukuto, J. 560
M.; Wink, D. A. *Proc. Natl. Acad. Sci. U.S.A.* **2003**, *100*, 9196. 561
(34) Paolucci, N.; Saavedra, W. F.; Miranda, K. M.; Martignani, C.; 562
Isoda, T.; Hare, J. M.; Espey, M. G.; Fukuto, J. M.; Feelisch, M.; Wink, 563
D. A.; Kass, D. A. *Proc. Natl. Acad. Sci. U.S.A.* **2001**, *98*, 10463. 564
(35) Adak, S.; Wang, Q.; Stuehr, D. J. *J. Biol. Chem.* **2000**, *275*, 565
33554. 566
(36) Schmidt, H. H. H. W.; Hofmann, H.; Schindler, U.; Shutenko, 567
Z. S.; Cunningham, D. D.; Feelisch, M. *Proc. Natl. Acad. Sci. U.S.A.* 568
1996, *93*, 14492. 569
(37) Feelisch, M.; Te Poel, M.; Zamora, R.; Deussen, A.; Moncada, S. 570
Nature **1994**, *368*, 62. 571
(38) Rousseau, D. L.; Li, D.; Couture, M.; Yeh, S.-R. *J. Inorg. Biochem.* 572
2005, *99*, 306. 573
(39) Ishimura, Y.; Gao, Y. T.; Panda, S. P.; Roman, L. J.; Masters, B. 574
S. S.; Weintraub, S. T. *Biochem. Biophys. Res. Commun.* **2005**, *338*, 543. 575
(40) Sabat, J.; Egawa, T.; Lu, C.; Stuehr, D. J.; Gerfen, G. J.; 576
Rousseau, D. L.; Yeh, S.-R. *J. Biol. Chem.* **2013**, *288*, 6095. 577
(41) Li, D.; Kabir, M.; Stuehr, D. J.; Rousseau, D. L.; Yeh, S.-R. *J. Am.* 578
Chem. Soc. **2007**, *129*, 6943. 579
(42) Donzelli, S.; Graham, M.; Flores-Santana, W.; Switzer, C. H.; 580
Yeh, G. C.; Huang, J.; Stuehr, D. J.; King, S. B.; Miranda, K. M.; Wink, 581
D. A.; Espey, M. G. *Free Radic. Biol. Med.* **2008**, *45*, 578. 582
(43) Kytzia, A.; Korth, H.; Sustmann, R.; Groot, H.; De Kirsch, M. 583
Chem.—Eur. J. **2006**, *12*, 8786. 584
(44) Armstrong, D. A.; Huie, R. E.; Lyman, S.; Koppenol, W. H.; 585
Merényi, G.; Neta, P.; Stanbury, D. M.; Steenken, S.; Wardman, P. 586
Bioinorg. React. Mech. **2013**, *9*, 59. 587
(45) Filipovic, M. R. M.; Miljkovic, J. L. J.; Nauser, T.; Royzen, M.; 588
Klos, K.; Shubina, T.; Koppenol, W. H.; Lippard, S. J.; Ivanović- 589
Burmazović, I.; Ivanovic, I. *J. Am. Chem. Soc.* **2012**, *134*, 12016. 590
(46) Miljkovic, J. L.; Kenkel, I.; Ivanović-Burmazović, I.; Filipovic, M. 591
R. Angew. Chem., Int. Ed. **2013**, *52*, 12061. 592
(47) Clyne, M. A. A.; Thrush, B. A. *Trans. Faraday Soc.* **1961**, *57*, 593
1305. 594
(48) Cashion, J. K.; Polanyi, J. C. *J. Chem. Phys.* **1959**, *30*, 317. 595
(49) Strausz, O. P.; Gunning, H. E. *Trans. Faraday Soc.* **1964**, *60*, 347. 596
(50) Kohout, F. C.; Lampe, F. W. *J. Am. Chem. Soc.* **1965**, *87*, 5795. 597
(51) Miranda, K. M.; Paolucci, N.; Katori, T.; Thomas, D. D.; Ford, 598
E.; Bartberger, M. D.; Espey, M. G.; Kass, D. A.; Feelisch, M.; Fukuto, 599
J. M.; Wink, D. A. *Proc. Natl. Acad. Sci. U.S.A.* **2003**, *100*, 9196. 600
(52) Porcheddu, A.; De Luca, L.; Giacomelli, G. *Synlett* **2009**, *13*, 601
2149. 602
(53) Heinecke, J. L.; Khin, C.; Pereira, J. C. M.; Suárez, S. A.; Iretskii, 603
A. V.; Doctorovich, F.; Ford, P. C. *J. Am. Chem. Soc.* **2013**, *135*, 4007. 604
(54) Álvarez, L.; Suarez, S. A.; Bikiel, D. E.; Reboucas, J. S.; Batinić- 605
Haberle, I.; Martí, M. A.; Doctorovich, F. *Inorg. Chem.* **2014**, *53*, 7351. 606

- 607 (55) Spasojevic, I.; Batini-Haberle, I.; Fridovich, I. *Nitric Oxide* **2000**,
608 *4*, 526.
- 609 (56) Benon, H. J.; Bielski, A.; Allen, O.; Schwarz, H. A. *J. Am. Chem.*
610 *Soc.* **1981**, *103*, 3516.
- 611 (57) Kirsch, M.; Büscher, A.-M.; Aker, S.; Schulz, R.; de Groot, H.
612 *Org. Biomol. Chem.* **2009**, *7*, 1954.
- 613 (58) Poderoso, J. J.; Carreras, M. C.; Schöpfer, F.; Lisdero, C. L.;
614 Riobó, N. A.; Giulivi, C.; Boveris, A. D.; Boveris, A.; Cadenas, E. *Free*
615 *Radic. Biol. Med.* **1999**, *26*, 925.
- 616 (59) Heinecke, J.; Ford, P. C. *Coord. Chem. Rev.* **2010**, *254*, 235.
- 617 (60) J. van der, Zee; P. J. A. van den, Broek *Free Radic. Biol. Med.*
618 **1998**, *25*, 282.
- 619 (61) Yenes, S.; Messeguer, A. *Tetrahedron* **1999**, *55*, 14111.
- 620 (62) May, J. M. *Free Radic. Biol. Med.* **2000**, *28*, 1421.
- 621 (63) Liu, X.; Miller, M. J.; Joshi, M. S.; Thomas, D. D.; Lancaster, J.
622 *R. Proc. Natl. Acad. Sci. U.S.A.* **1998**, *95*, 2175.
- 623 (64) Kamga, C.; Krishnamurthy, S.; Shiva, S. *Nitric Oxide* **2012**, *26*,
624 251.
- 625 (65) Gupta, K. J.; Igamberdiev, A. U.; Manjunatha, G.; Segu, S.;
626 Moran, J. F.; Neelawarne, B.; Bauwe, H.; Kaiser, W. M. *Plant Sci.* **2011**,
627 *181*, 520.
- 628 (66) Shiva, S.; Huang, Z.; Grubina, R.; Sun, J.; Ringwood, L. A.;
629 MacArthur, P. H.; Xu, X.; Murphy, E.; Darley-Usmar, V. M.; Gladwin,
630 M. T. *Circ. Res.* **2007**, *100*, 654.
- 631 (67) Chouchani, E. T.; Methner, C.; Nadtochiy, S. M.; Logan, A.;
632 Pell, V. R.; Ding, S.; James, A. M.; Cochemé, H. M.; Reinhold, J.;
633 Lilley, K. S.; Partridge, L.; Fearnley, I. M.; Robinson, A. J.; Hartley, R.
634 C.; Smith, R. A. J.; Krieg, T.; Brookes, P. S.; Murphy, M. P. *Nat. Med.*
635 **2013**, *19*, 753.